A Hybrid Power Line/Wireless Dual-Hop System With Energy Harvesting Relay

Victor Fernandes, H. Vincent Poor, *Fellow, IEEE*, and Moisés V. Ribeiro, *Senior Member, IEEE*

***Abstract*—This paper investigates the benefits that energy harvesting (EH) can offer to increase energy efficiency in hybrid power line/wireless data communication systems for smart grid (SG) and Internet of Things (IoT) applications. In this regard, the ergodic achievable data rates of a hybrid power line/wireless dual-hop system (H2HS) model that uses EH strategies and the amplify-and-forward protocol at the relay node are considered. Also, four approaches for performing EH in the H2HS system are discussed. Performance comparisons among the H2HS, a dual-hop power line and a dual-hop wireless systems are performed by adopting four simulation settings, covering the combinations of optimal or uniform power allocation together with colored or white additive noise at the output of the power line channel. Numerical results show that the H2HS model with the power splitting EH strategy outperforms the other models. Moreover, if the transmission power of the source node is high, then the case with additive colored noise at the received power line signal can result in higher achievable data rates in comparison to the white noise case. Overall, the H2HS system making use of an EH strategy has the potential to increase the sustainability and energy efficiency in data communications for SG and IoT applications.**

***Index Terms*—Achievable data rate, cooperative communication, energy harvesting (EH), power line communication (PLC), wireless communication (WLC).**

I. Introduction

THE modernization of data communication infrastructures to fulfill the needs and demands of smart grids (SGs) and the Internet of Things (IoT) can bring several benefits. However, to accomplish this aim, it is necessary to have flexibility to ensure reliability, since no single data communication technology covers all possible scenarios [1], [2]. In this regard, the mutual uses of power line communication (PLC) [3]–[7], wireless communication (WLC), and visible light communication (VLC) are being pursued [8]–[10]. Also, cooperative communication concepts based on relaying and combining techniques at physical and link layers are being investigated [11]–[13] for exploiting the existing diversity among PLC, WLC, and VLC channels. Furthermore, [14]–[16] showed that communications systems based on the use of hybrid power line/wireless channels can offer improved reliability or higher data rate in comparison with nonhybrid channels, even when this system loses a data communication link or a node communication interface [17].

Additionally, the increasing demand for more energy efficient and smarter data communication devices, is motivating research efforts on how to effectively and efficiently take advantage of the energy of the received signal for powering a transceiver. As stated in [18], one of the dominant barriers to implement IoT is supplying enough energy to operate the network in a self-sufficient manner. Among several initiatives to deal with this challenging issue, the concept of energy harvesting (EH) is being increasingly investigated. Initially, the research efforts related to EH were focused on WLC. Recently, research attention in this area has turned to PLC because its combination with WLC and VLC will play a pivotal role in the future of SG and IoT applications.

In particular, when energy efficiency is brought to the center of discussions about the evolution of data communication technologies for assisting massive deployment of SG and IoT technologies, the EH strategies [19] start to play an important role in providing the appropriate tools in the reuse of the expended energy for transmitting information through data communication media. In fact, the successful implementation of EH strategies may allow a data communication node to power itself by harvesting energy from the received signal, which was transmitted by another node and, thus, the end of battery life can be postponed or, eventually, eliminated. In the era of SG and IoT, the EH strategies may be of fundamental importance for energy supply and information exchange among numerous low-power devices [20] that make use of an intermittent or unavailable energy supply, which can occur due to the design of the device, failure of the power supply, and/or the end of stored energy. As a result, current applications related to SGs, the IoT and novel ones associated with smart cities and Industry 4.0, such as smart home, healthcare, surveillance, transportation [18], smart metering [21], monitoring and control [22], smart mining, and industrial sensor networks [23] can take advantages of it.

In this regard, [24] focused on the tradeoff between the harvested energy and the WLC channel capacity. In the sequel, it was extended to address frequency-selective channels [25].

Manuscript received February 5, 2018; revised July 4, 2018; accepted July 17, 2018. Date of publication July 27, 2018; date of current version November 14, 2018. This work was supported in part by CNPq, in part by CAPES, in part by FAPEMIG, in part by FINEP, in part by INERGE, in part by Smarti9 LTD., and in part by the U.S. National Science Foundation under Grant CNS-1702808. *(Corresponding author: Victor Fernandes.)*

V. Fernandes is with the Department of Electrical Engineering, Federal University of Juiz de Fora, Juiz de Fora 36036-330, Brazil (e-mail: victor.fernandes@engenharia.ufjf.br).

H. V. Poor is with the Department of Electrical Engineering, Princeton University, Princeton, NJ 08544 USA (e-mail: poor@princeton.edu).

M. V. Ribeiro is with the Department of Electrical Engineering, Federal University of Juiz de Fora, Juiz de Fora 36036-330, Brazil, and also with Smarti9 LTD., Juiz de Fora, 36036-330, Brazil (e-mail: mribeiro@ieee.org).

Digital Object Identifier 10.1109/JIOT.2018.2860458

Moreover, [24] and [25] considered that the receiver could simultaneously decode the information and perform EH, which may not be a practical approach. Furthermore, [26] outlined two EH relaying protocols, namely, time switching (TS) and power splitting (PS). In the former, the relay shares the time between EH and data communication tasks, while in the latter, the relay simultaneously splits the power between EH and data communication ones. Also, [26] showed that TS outperforms PS in terms of throughput and data rates for low signal-to-noise conditions if amplify-and-forward (AF) relaying-based cooperative communication is adopted. Moreover, [27] provided a performance comparison between TS and PS strategies, by means of the rate-energy region, considering a multiple-input and multiple-output broadcast system. Furthermore, [28] investigated the power allocation strategies for a decode-and-forward (DF) EH relaying system with multiple source-destination pairs and [29] extended this analysis when an interfering signal is present.

Focusing on the EH strategies for PLC systems, a few works have addressed this topic, such as [30] and [31]. More specifically, [30] considered a dual-hop DF PLC system with TS at the relay node and showed that it is possible to provide energy efficiency improvements of more than 30% in comparison to the conventional DF relaying scheme when energy is harvested from the additive impulsive noise in the power lines. In the sequel, [31] considered a dual-hop AF PLC system with TS at the relay node and showed that as the noise becomes more impulsive, more energy will be harvested and the EH time factor was recognized as a key parameter to optimize the system performance.

It is important to emphasize that previous works highlighted the benefits of using EH strategies together with relays for individual WLC or PLC system. However, neither of them have addressed the benefits associated with the use of EH strategies together with the hybrid power line/wireless system, nor have they paid attention to the typical frequency bands that are anticipated for use by SG and IoT technologies.

Aiming to deal with the aforementioned issues and to increase the lifetimes, energy efficiency and flexibility of transceivers, we focus on the association among cooperative communication, the hybridism concept, and EH for narrowband or low-data-rate transceivers that are suitable for SG and IoT applications. In this context, SG and IoT devices can eventually make use of intermittent energy supplies, do not have energy supplies, or lose their energy supplies due to unexpected failures.

In this regard, the main contributions of this paper can be summarized as follows.

1) Formulation of the ergodic achievable data rates of the hybrid power line/wireless dual-hop system (H2HS) model when the TS, PS, or the proposed hybrid TS (HTS) strategy together with the AF protocol and maximal ratio combining (MRC) technique are applied at the relay node.
2) Introduction and discussion of four different EH approaches: a) the H2HS system harvests the energy at the relay node only from the wireless signal using hybrid time switching (HTS) (Approach A); b) only from the power line signal using HTS (Approach B); c) from both power line and wireless signals using TS (Approach C); and d) from both power line and wireless signals using PS (Approach D).
3) Evaluation and performance comparisons among H2HS, power line dual-hop system (P2HS) and wireless dual-hop system (W2HS) under four simulation settings. These settings cover important scenarios for evaluation purposes.

Our numerical results lead us to the following conclusions.

1) For high transmission power at the source node, the nonflat power spectral density (PSD) feature of the PLC additive noise can increase the achievable data rate gains in comparison with the flat PSD assumption of the additive noise, something that agrees with [30] and [31]. Regardless of the simulation setting, the H2HS system always outperforms P2HS and W2HS systems in terms of EH.
2) For any H2HS systems, the optimal values of TS and PS factors yield better performance in favor of the PS strategy rather than TS. Also, Approaches A and B are shown to provide upper bounds for Approach C regardless of the value of TS and PS factors and the listed settings. Last, but not least, Approach D is more appealing for SG and IoT applications because of its resilience against the types of transmission power allocation and the intrinsic characteristics of PLC and WLC channels.

The rest of this paper is organized as follows. Section II introduces the H2HS model and formulates the investigated problem. Section III briefly describes the TS and PS strategies and deals with the ergodic achievable data rates of the four approaches in the H2HS model. Section IV discusses the numerical results; and, finally, Section V states our concluding remarks.

II. Problem Formulation

The H2HS model is shown in Fig. 1. It is composed of parallel power line and wireless dual-hop systems. In this model, each node makes use of power line and wireless media to transmit signals among source (S), relay (R), and destination (D) nodes. The R node operates in half-duplex mode and it uses the MRC technique to combine the signals received from the S node through the power line and wireless media. Also, it makes use of the AF protocol to forward the amplified version of the received signal to the D node. In this model, the only source of power at the R node comes from the energy harvested from the signals received by the R node.

According to Fig. 1, the S node transmits the source information to the R node through the wireless and power line channels during the first phase. During the second phase, the R node combines the received information and forwards it to the D node. In this context, we assume that the direct (S $\rightarrow$ D) link is not feasible due to the high attenuation associated with the relatively large distance between S and D nodes. The transmission power spent at the S node is $P_{\mathrm{S}} = P_1^P + P_1^W \geq 0$, in which $P_1^P \geq 0$ and $P_1^W \geq 0$ are the transmission power allocated to the power line and wireless (S $\rightarrow$ R) node communication

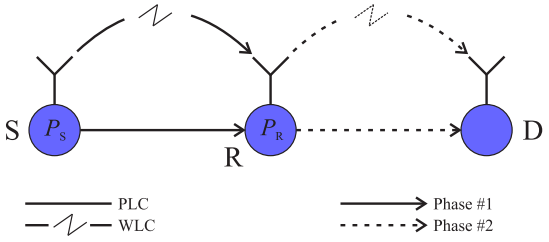

Fig. 1. H2HS model.

interfaces, respectively. Similarly, $P_{\mathrm{R}} = P_2^P + P_2^W \geq 0$ is the transmission power obtained from the energy harvested from the signals received by the R node, where $P_2^P \geq 0$ and $P_2^W \geq 0$ are the transmission power allocated to the power line and wireless (R $\rightarrow$ D) node communication interfaces, respectively. Furthermore, we assume that $P = P_{\mathrm{S}} + P_{\mathrm{R}}$ is the total transmission power. Note that $P_t^q \geq 0$ is the transmission power allocated to the communication interface associated with the qth communication medium in the tth phase, in which $q \in \{P, W\}$ refers to power line or wireless medium and $t \in \{1, 2\}$ denotes the first and second phases, respectively.

Moreover, the power line and wireless channels are assumed to be linear and time varying among different phases. Also, both of them remain time invariant during one phase. In other words, the discrete-time representations of channel impulse responses, for a given N-block symbol duration (one phase duration), are denoted by $\{h_\ell^q[n]\}_{n=0}^{L_\ell^q-1}$, in which L_ℓ^q are their lengths, $\max_\ell\{L_\ell^q\} \leq L_{\max}, \forall q, \ell$, and $\ell \in \{\mathrm{SR}, \mathrm{RD}\}$ refers to the SR or RD link.

In [15], it was shown that power line and wireless single-relay channels could be modeled as two parallel linear Gaussian relay channels (LGRCs) (see [32]). In this regard and similar to [15], we assume that the H2HS is also modeled by two parallel LGRCs (one for power line and one for wireless), during one N-block symbol duration. In other words, the LGRC assumption is also applied to the power line and wireless dual-hop systems. Moreover, we assume that both power line and wireless channels are statistically independent of each other and from the additive noise. Furthermore, direct data communication from the S node to the D node is not possible.

In this setting, we define the N-block memoryless channel as the channel, where the outputs over any N-block transmission are independent of channel inputs and noise samples from previous or subsequent N-block transmissions, for $N > L_{\max}$ [33]. Also, we define the N-block memoryless circular Gaussian relay channel (N-CGRC) as the N-block LGRC (N-LGRC) switching the linear convolution operation associated with the LGRC for the circular convolution associated with the CGRC formulation. Now, and most important, as [32] states, the direct computation of the channel capacity of the N-LGRC is challenged by the presence of interblock interference due to the fact that the channel impulse responses have memory and the additive noises are correlated random processes. As addressed in [33], the channel capacity of the N-LGRC tends to be equal to that of the N-CGRC as $N \rightarrow \infty$. The N-CGRC model avoids interblock interference by converting the linear convolution of an N-LGRC into a circular convolution, which is a distinct advantage for analytical and numerical computation purposes.

In this sense, let the discrete-time vectorial representation of the impulse response of the channel associated with the qth communication medium and the ℓth link during one N-block symbol duration be $\mathbf{h}_\ell^q = [h_\ell^q[0], h_\ell^q[1], \ldots, h_\ell^q[L_\ell^q - 1]]^T$; then $\mathbf{H}_\ell^q = [H_\ell^q[0], H_\ell^q[1], \ldots, H_\ell^q[N-1]]^T$ is the N-length discrete Fourier transform of the channel impulse response of the power line or wireless channel such that $\mathbf{H}_\ell^q = \boldsymbol{\mathcal{F}}[\mathbf{h}_\ell^q, \mathbf{0}_{N-L_\ell^q}]^T$, in which $\boldsymbol{\mathcal{F}}$ is the $N \times N$ discrete Fourier transform matrix, $\mathbf{0}_{M_0}$ is an M_0-length column vector of all zeros and N is the number of subchannels. We also define the diagonal matrices $\boldsymbol{\mathcal{H}}_\ell^q \triangleq \mathrm{diag}\{H_\ell^q[0], H_\ell^q[1], \ldots, H_\ell^q[N-1]\}$, and similarly, $\boldsymbol{\Lambda}_{|\boldsymbol{\mathcal{H}}_\ell^q|^2} \triangleq \mathrm{diag}\{|H_\ell^q[0]|^2, |H_\ell^q[1]|^2, \ldots, |H_\ell^q[N-1]|^2\}$. Moreover, the joint probability $p(|H_\ell^q[0]|^2, |H_\ell^q[1]|^2, \ldots, |H_\ell^q[N-1]|^2) = p(|H_\ell^q[0]|^2)p(|H_\ell^q[1]|^2)\ldots p(|H_\ell^q[N-1]|^2)$ because we assume that $H_\ell^q[i]$ and $H_\ell^q[j]$, $\forall i \neq j$ are independent random variables.

The vectorial representation of a symbol, after digital modulation in the frequency domain, is given by $\mathbf{X} \in \mathbb{C}^{N\times 1}$, while $\mathbf{V}_\ell^q \in \mathbb{C}^{N\times 1}$ is the vectorial representation of the additive noise in the frequency domain for the qth communication medium associated with the ℓth link. Moreover, we consider that $\mathbb{E}\{\mathbf{X}\} = 0$, $\mathbb{E}\{\mathbf{X}\mathbf{X}^\dagger\} = \boldsymbol{\Lambda}_{\sigma_X^2} = \mathbf{I}_N$, in which $\mathbf{I}_{M_1}$ denotes the $M_1 \times M_1$ identity matrix, $\mathbb{E}\{\cdot\}$ denotes expectation and $\dagger$ denotes the conjugate transpose operator. Also, $\mathbb{E}\{\mathbf{V}_\ell^q\} = 0$ and $\mathbb{E}\{\mathbf{V}_\ell^q\mathbf{V}_\ell^{q\dagger}\} = \boldsymbol{\Lambda}_{\sigma^2_{\mathbf{V}_\ell^q}} = \mathrm{diag}\{\sigma^2_{\mathbf{V}_\ell^q}[0], \sigma^2_{\mathbf{V}_\ell^q}[1], \ldots, \sigma^2_{\mathbf{V}_\ell^q}[N-1]\}$. In addition, we have $\boldsymbol{\Lambda}_{P_t^q} = \mathrm{diag}\{P_{t,0}^q, P_{t,1}^q, \ldots, P_{t,N-1}^q\}$ as a matrix representation of power allocation, so that $\mathrm{Tr}(\boldsymbol{\Lambda}_{P_t^q}) = P_t^q$, where $\mathrm{Tr}(\cdot)$ denotes the trace operator. Therefore, $\boldsymbol{\Lambda}_{\sqrt{P_t^q}} = \mathrm{diag}\{\sqrt{P_{t,0}^q}, \sqrt{P_{t,1}^q}, \ldots, \sqrt{P_{t,N-1}^q}\}$ denotes the amplitude in the frequency domain of the transmitted symbol through the qth communication medium at the tth phase.

Due to the intrinsic characteristics of both power line and wireless channels and the need for guaranteeing fairness and exploiting the existing diversity between them, we assume that $\|\mathbf{h}_\ell^P\|^2 = \|\mathbf{h}_\ell^W\|^2 = \gamma$ and $P_{v,\ell}^W = P_{v,\ell}^P$, in which $\|\cdot\|$ denotes the 2-norm. Note that $\|\mathbf{h}_\ell^q\|^2$ is the channel energy associated with the qth communication medium and the ℓth link, while $P_{v,\ell}^q$ denotes the power of the additive noise associated with the qth communication medium and the ℓth link.

Given the aforementioned formulation, the following research question arises: *can an H2HS yield higher achievable data rates than the separate use of nonhybrid two-hop systems (P2HS or W2HS) when a sum power constraint applies and EH is adopted at the R node*? The answer to this question gives guidance for the development of IoT technologies that are sustainable and efficient in the energy consumption sense. The following sections address the answer to this question.

III. Proposed Approaches for EH in the H2HS Model

This section describes the four approaches for performing EH in the H2HS model. In general, they differ from each other in terms of the time interval usage before the second phase. In this context, we first formulate the ergodic achievable data

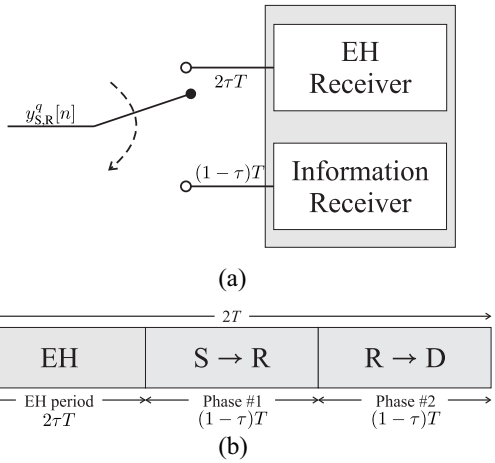

Fig. 2. (a) Block diagram of the TS strategy at the R node, and (b) illustration of the key TS parameters.

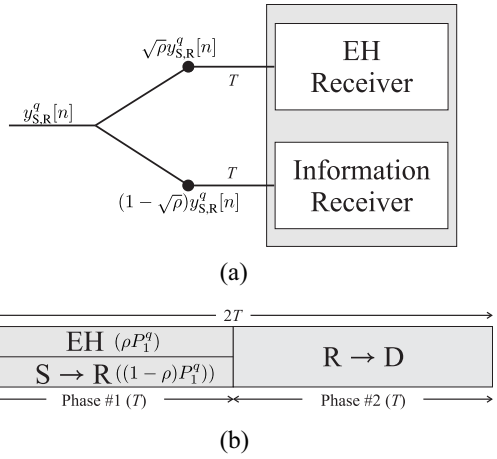

Fig. 3. (a) Block diagram of the PS strategy at the R node, and (b) illustration of the key PS parameters.

rate of the H2HS model without EH and then the ergodic achievable data rate of these four approaches. This roadmap allows us to straightforwardly derive the four approaches from the H2HS model.

To do so, the TS and PS strategies are concisely reviewed from the EH perspective in Section III-A. In the sequel, Section III-B formulates the ergodic achievable data rate of the H2HS model without the use of EH. Finally, Section III-C details Approaches A, B, C, and D and how they are derived from the ergodic achievable data rate of the H2HS model.

A. TS and PS Strategies

First of all, assume that the harvested energy is equally split between both power line and wireless interfaces during the second phase. Also, we make the somewhat pessimistic assumption that only the energy of the received signal is utilized for EH [26], [27]. In other words, the energy associated with the additive noise is not taken into account.

According to Fig. 2, the TS strategy considers that the R node uses the time period of $2\tau T$ for EH, $(1-\tau)T$ for the S $\rightarrow$ R node communication during the first phase, and the remaining $(1-\tau)T$ for the R $\rightarrow$ D node communication during the second phase, in which T is a time interval and $0 < \tau < 1$ is the TS factor. In this regard, the energy harvested from the received signal associated with the qth communication medium at the R node is given by

$$E_{\mathrm{R}}^q = 2\eta\tau P_1^q \|\mathbf{h}_{\mathrm{SR}}^q\|^2 T \tag{1}$$

in which $0 < \eta \leq 1$ is the energy conversion efficiency [19]. Also, using (1), the transmission power for data communication from the R node, through the qth communication medium, to the D node is expressed as

$$P_2^q = \frac{E_{\mathrm{R}}^q}{(1-\tau)T} = \frac{2\eta\tau P_1^q \|\mathbf{h}_{\mathrm{SR}}^q\|^2}{(1-\tau)}. \tag{2}$$

On the other hand, in the PS strategy (see Fig. 3), the received energy during the first phase is split between S $\rightarrow$ R data communication and EH. This division respects the splitting factor, ρ. In other words, the R node harvests the energy from the received signal $\sqrt{\rho}y^q_{\mathrm{S,R}}[n]$, which is associated with the qth communication medium. The remaining energy, which is associated with $(1-\sqrt{\rho})y^q_{\mathrm{S,R}}[n]$, is used for recovering the transmitted signal at the R node. Therefore, the harvested energy at the R node from the qth communication medium is given by

$$E_{\mathrm{R}}^q = \eta\rho P_1^q \|\mathbf{h}_{\mathrm{SR}}^q\|^2 T \tag{3}$$

in which $0 < \rho < 1$. Furthermore, using (3), the available transmission power at the R node for data communication with the D node, through the qth communication medium, is expressed as

$$P_2^q = \frac{E_{\mathrm{R}}^q}{T} = \eta\rho P_1^q \|\mathbf{h}_{\mathrm{SR}}^q\|^2. \tag{4}$$

B. Achievable Data Rates

This section deals with the derivation of a closed-form expression for the ergodic achievable data rate of the H2HS model. To accomplish this aim, we adopt the AF cooperative protocol [11], [12], [15], [26], [31] and the MRC technique [12].

Now, we can state that the frequency domain vectorial representation of a symbol at the output of the qth communication medium associated with the SR link, during the first phase, is given by

$$\mathbf{Y}_{\mathrm{SR}}^q = \mathbf{\Lambda}_{\sqrt{P_1^q}} \mathcal{H}_{\mathrm{SR}}^q \mathbf{X} + \mathbf{V}_{\mathrm{SR}}^q. \tag{5}$$

Note that the AF protocol allows the further transmission of the received symbol by the R node to the D node using an amplification factor, which is related to the power allocated to the R node during the second phase. Mathematically, the vectorial frequency domain representation of the symbol at the output of the qth communication medium associated with the RD link is given by [15]

$$\mathbf{Y}_{\mathrm{RD,AF}}^q = \mathbf{\Lambda}_{\sqrt{P_2^q}} \mathcal{H}_{\mathrm{RD}}^q \mathbf{X}_{\mathrm{R}} + \mathbf{V}_{\mathrm{RD}}^q \tag{6}$$

in which $\mathbf{X}_{\mathrm{R}} = \mathbf{\Lambda}^{-1}_{\sigma_{\mathbf{Y}_{\mathrm{SR}}}} (\mathbf{D}^{P}\mathbf{Y}^{P}_{\mathrm{SR}} + \mathbf{D}^{W}\mathbf{Y}^{W}_{\mathrm{SR}})$ and

$$\mathbf{\Lambda}_{\sigma^2_{\mathbf{Y}_{\mathrm{SR}}}} = \left|\mathbf{D}^{P}\mathbf{\Lambda}_{\sqrt{P^{P}_{1}}}\mathcal{H}^{P}_{\mathrm{SR}} + \mathbf{D}^{W}\mathbf{\Lambda}_{\sqrt{P^{W}_{1}}}\mathcal{H}^{W}_{\mathrm{SR}}\right|^2 + \left|\mathbf{D}^{P}\right|^2\mathbf{\Lambda}_{\sigma^2_{\mathbf{V}^{P}_{\mathrm{SR}}}} + \left|\mathbf{D}^{W}\right|^2\mathbf{\Lambda}_{\sigma^2_{\mathbf{V}^{W}_{\mathrm{SR}}}} \tag{7}$$

where $\mathbf{D}^{q} = \mathbf{\Lambda}_{\sqrt{P^{q}_{1}}}\mathcal{H}^{q\ \dagger}_{\mathrm{SR}}\mathbf{\Lambda}^{-1}_{\sigma^2_{\mathbf{V}^{q}_{\mathrm{SR}}}}$ [12]. From (5) and (6), the vectorial representation of the received symbol at the R node can be expressed by (8) at the bottom of this page.

Now, let $f(\mathbf{Z})$ denote the entropy of a random vector $\mathbf{Z}$. Also, let $\mathbf{Y} \in \mathbb{C}^{2N\times 1}$ be the received symbol at the D node after the two phases; then the mutual information between the transmitted and received symbols is [12], [15]

$$I(\mathbf{X}, \mathbf{Y}) = f(\mathbf{Y}) - f(\mathbf{BV}). \tag{9}$$

Based on the assumption that $\mathbf{X}$ is Gaussian distributed, we have

$$f(\mathbf{Y}) = \log_2\Big[(\pi e)^{2N}\det(\mathbf{R}_{\mathbf{YY}})\Big] \tag{10}$$

and, due to the Gaussianity of the additive noise, we write

$$f(\mathbf{BV}) = \log_2\Big[(\pi e)^{2N}\det\Big(\mathbf{B}\mathbf{R}_{\mathbf{VV}}\mathbf{B}^{\dagger}\Big)\Big] \tag{11}$$

where $\mathbf{R}_{\mathbf{YY}} = \mathbb{E}\{\mathbf{Y}\mathbf{Y}^{\dagger}\} = \mathbf{A}\mathbf{R}_{\mathbf{XX}}\mathbf{A}^{\dagger} + \mathbf{B}\mathbf{R}_{\mathbf{VV}}\mathbf{B}^{\dagger}$, $\mathbf{R}_{\mathbf{XX}} = \mathbb{E}\{\mathbf{X}\mathbf{X}^{\dagger}\}$, and $\mathbf{R}_{\mathbf{VV}} = \mathbb{E}\{\mathbf{V}\mathbf{V}^{\dagger}\}$. On defining $\mathbf{C}_{\mathrm{AF}} = \mathbf{A}\mathbf{R}_{\mathbf{XX}}\mathbf{A}^{\dagger}$ and $\mathbf{D}_{\mathrm{AF}} = \mathbf{B}\mathbf{R}_{\mathbf{VV}}\mathbf{B}^{\dagger}$, in which $\mathbf{C}_{\mathrm{AF}}$ and $\mathbf{D}_{\mathrm{AF}}$ are given by (12) and (13), as shown at the bottom of the next page, respectively, from (9), the mutual information is given by

$$I(\mathbf{X}, \mathbf{Y}) = \log_2\Big[\det\Big(\mathbf{I}_{2N} + \mathbf{C}_{\mathrm{AF}}\mathbf{D}^{-1}_{\mathrm{AF}}\Big)\Big]. \tag{14}$$

As a result, the ergodic achievable data rate of the H2HS model adopting AF and MRC at the R node, which uses $2T$ time slots and N sub-bands, is given by

$$C^{\mathrm{H2HS}} = \mathbb{E}_{\mathbf{H}^{P}_{\ell},\mathbf{H}^{W}_{\ell}}\left\{\max_{\mathbf{\Lambda}_P}\frac{B_W}{N}\log_2\left[\det\Big(\mathbf{I}_{2N} + \mathbf{C}_{\mathrm{AF}}\mathbf{D}^{-1}_{\mathrm{AF}}\Big)\right]\right\} \tag{15}$$

subject to $\mathrm{Tr}(\mathbf{\Lambda}_P) \leq P$, where $\mathbf{\Lambda}_P = \mathrm{diag}\Big\{\mathbf{\Lambda}_{P^{P}_{1}}, \mathbf{\Lambda}_{P^{W}_{1}}, \mathbf{\Lambda}_{P^{P}_{2}}, \mathbf{\Lambda}_{P^{W}_{2}}\Big\}$, B_W and $\mathbb{E}_{\mathbf{H}^{P}_{\ell},\mathbf{H}^{W}_{\ell}}\{.\}$ are the frequency bandwidth and the expectation operation related to both power line and wireless channels, respectively.

C. Proposed Approaches

The proposed four EH approaches in the H2HS model are depicted in Fig. 4. Basically, these approaches refer to distinct approaches to harvesting energy from the H2HS model by exploiting the PS and TS strategies and the existing diversity in the hybrid data communication channel (i.e., parallel use of PLC and WLC channels). Based on (12) and (13), closed-form expressions for the ergodic achievable data rates of these approaches are concisely obtained as follows.

1) *Approach A:* During the first phase, the energy at the R node is harvested only from the signal associated with the wireless SR link, while the power line SR link is used for performing the S $\rightarrow$ R data communication. To evaluate the achievable data rate, the terms related to the wireless SR link (i.e., $\mathbf{D}^{W}$, $\mathbf{\Lambda}_{\sqrt{P^{W}_{1}}}$ and $\mathcal{H}^{W}_{\mathrm{SR}}$) are removed from (12) and (13). Also, 2τ multiplies $\mathbf{\Lambda}_{P^{P}_{1}}$, while $2(1-\tau)$ multiplies $\mathbf{\Lambda}_{P^{P}_{2}}$ and $\mathbf{\Lambda}_{P^{W}_{2}}$. Further, the EH value is that harvested from the wireless signal. In other words, the total harvested energy is $E_{\mathrm{R}} = E^{W}_{\mathrm{R}} = 2\eta\tau P^{W}_{1}\|\mathbf{h}^{W}_{\mathrm{SR}}\|^2 T$.
2) *Approach B:* This is the opposite of Approach A. In particular, energy is harvested from the power line signal associated with the SR link, while the wireless SR link is used for carrying out S $\rightarrow$ R data communication, during the first phase. To evaluate the achievable data rate, the terms related to the power line SR link (i.e., $\mathbf{D}^{P}$, $\mathbf{\Lambda}_{\sqrt{P^{P}_{1}}}$ and $\mathcal{H}^{P}_{\mathrm{SR}}$) are removed from (12) and (13). Moreover, 2τ multiplies $\mathbf{\Lambda}_{P^{W}_{1}}$, while $2(1-\tau)$ multiplies $\mathbf{\Lambda}_{P^{P}_{2}}$ and $\mathbf{\Lambda}_{P^{W}_{2}}$. As a result, the total harvested energy is $E_{\mathrm{R}} = E^{P}_{\mathrm{R}} = 2\eta\tau P^{P}_{1}\|\mathbf{h}^{P}_{\mathrm{SR}}\|^2 T$. The EH strategy used in Approaches A and B is called the HTS strategy.
3) *Approach C:* In this approach, EH is carried out in the power line and wireless signals associated with SR links by using the TS strategy. Thus, the signals associated with both power line and wireless SR links are used for harvesting energy during the EH period and, after that, they are used for performing S $\rightarrow$ R data communication based on the use of the TS factor. To evaluate the achievable data rate, a change is made in (12) and (13) by multiplying the terms $\mathbf{\Lambda}_{P^{P}_{1}}$, $\mathbf{\Lambda}_{P^{P}_{2}}$, $\mathbf{\Lambda}_{P^{W}_{1}}$, and $\mathbf{\Lambda}_{P^{W}_{2}}$ by $(1-\tau)$. Also, the total harvested energy is given by $E_{\mathrm{R}} = E^{P}_{\mathrm{R}} + E^{W}_{\mathrm{R}} = 2\eta\tau T(P^{P}_{1}\|\mathbf{h}^{P}_{\mathrm{SR}}\|^2 + P^{W}_{1}\|\mathbf{h}^{W}_{\mathrm{SR}}\|^2)$.
4) *Approach D:* This approach is based on the simultaneous use of power line and wireless signals received by the R node. From these signals, EH and S $\rightarrow$ R

$$\begin{aligned}\mathbf{Y} &= \left[\mathbf{Y}^{P}_{\mathrm{SRD,AF}}{}^{T}, \mathbf{Y}^{W}_{\mathrm{SRD,AF}}{}^{T}\right]^{T}\\ &= \begin{bmatrix}\mathbf{\Lambda}_{\sqrt{P^{P}_{2}}}\mathcal{H}^{P}_{\mathrm{RD}}\mathbf{\Lambda}^{-1}_{\sigma_{\mathbf{Y}_{\mathrm{SR}}}}\left(\mathbf{D}^{P}\mathbf{\Lambda}_{\sqrt{P^{P}_{1}}}\mathcal{H}^{P}_{\mathrm{SR}} + \mathbf{D}^{W}\mathbf{\Lambda}_{\sqrt{P^{W}_{1}}}\mathcal{H}^{W}_{\mathrm{SR}}\right)\\ \mathbf{\Lambda}_{\sqrt{P^{W}_{2}}}\mathcal{H}^{W}_{\mathrm{RD}}\mathbf{\Lambda}^{-1}_{\sigma_{\mathbf{Y}_{\mathrm{SR}}}}\left(\mathbf{D}^{P}\mathbf{\Lambda}_{\sqrt{P^{P}_{1}}}\mathcal{H}^{P}_{\mathrm{SR}} + \mathbf{D}^{W}\mathbf{\Lambda}_{\sqrt{P^{W}_{1}}}\mathcal{H}^{W}_{\mathrm{SR}}\right)\end{bmatrix}\mathbf{X} + \begin{bmatrix}\mathbf{\Lambda}_{\sqrt{P^{P}_{2}}}\mathcal{H}^{P}_{\mathrm{RD}}\mathbf{\Lambda}^{-1}_{\sigma_{\mathbf{Y}_{\mathrm{SR}}}}\mathbf{D}^{P} & \mathbf{I}_N & \mathbf{\Lambda}_{\sqrt{P^{P}_{2}}}\mathcal{H}^{P}_{\mathrm{RD}}\mathbf{\Lambda}^{-1}_{\sigma_{\mathbf{Y}_{\mathrm{SR}}}}\mathbf{D}^{W} & 0\\ \mathbf{\Lambda}_{\sqrt{P^{W}_{2}}}\mathcal{H}^{W}_{\mathrm{RD}}\mathbf{\Lambda}^{-1}_{\sigma_{\mathbf{Y}_{\mathrm{SR}}}}\mathbf{D}^{P} & 0 & \mathbf{\Lambda}_{\sqrt{P^{W}_{2}}}\mathcal{H}^{W}_{\mathrm{RD}}\mathbf{\Lambda}^{-1}_{\sigma_{\mathbf{Y}_{\mathrm{SR}}}}\mathbf{D}^{W} & \mathbf{I}_N\end{bmatrix}\mathbf{V}\\ &= \mathbf{A}\mathbf{X} + \mathbf{B}\mathbf{V}\end{aligned}$$

where

$$\mathbf{V} = \left[\mathbf{V}^{P}_{\mathrm{SR}}{}^{T}\mathbf{V}^{P}_{\mathrm{RD}}{}^{T}\mathbf{V}^{W}_{\mathrm{SR}}{}^{T}\mathbf{V}^{W}_{\mathrm{RD}}{}^{T}\right]^{T} \tag{8}$$

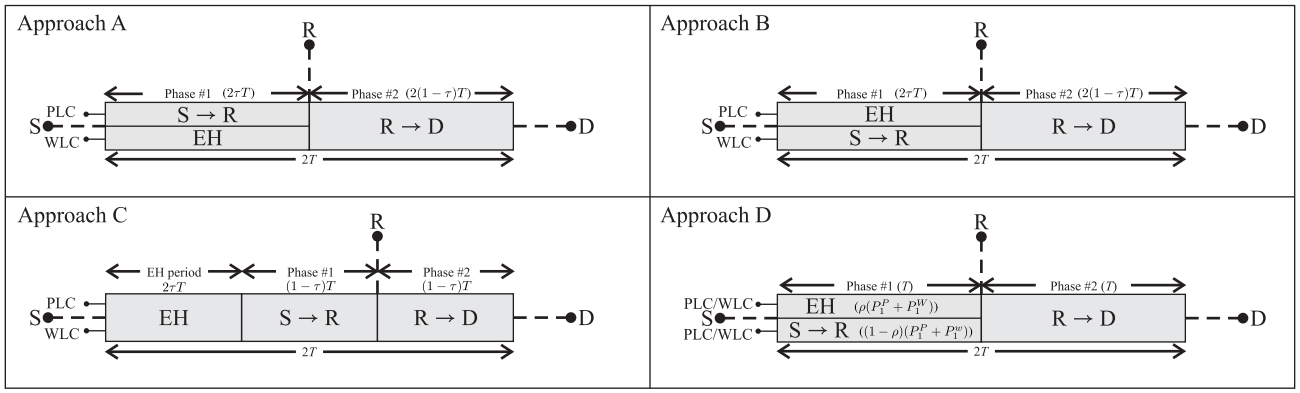

Fig. 4. Block diagrams of Approach A (HTS), Approach B (HTS), Approach C (TS), and Approach D (PS).

data communication are accomplished by adopting PS. To evaluate the achievable data rate, (12) and (13) are changed by multiplying the terms $\mathbf{\Lambda}_{P_1^P}$ and $\mathbf{\Lambda}_{P_1^W}$ by $(1-\rho)$ and the harvested energy is expressed as $E_{\mathrm{R}} = E_{\mathrm{R}}^P + E_{\mathrm{R}}^W = \eta\rho T(P_1^P\|\mathbf{h}_{\mathrm{SR}}^P\|^2 + P_1^W\|\mathbf{h}_{\mathrm{SR}}^W\|^2)$.

IV. Numerical Results

In order to carry out numerical simulations regarding the H2HS model, we assume that the signal transmission occurs in the industrial, scientific, and medical (ISM) frequency band for WLC and the low-frequency band for PLC. The narrowband-PLC (NB-PLC) is standardized to operate in the frequency band from 0 up to 500 kHz [34]. For the sake of a fair comparison, the low-power radio frequency (LP-RF) wireless data transmission occupies a bandwidth equal to 500 kHz in the frequency band between 915 and 915.5 MHz. Furthermore, a large value of N is used such that the subchannel gains and PSD of the additive noise are flat within each subchannel. This choice is useful to accomplish realizable numerical simulations.

Note that $P_{\mathrm{S}} \in \{1, 100\}$ mW is adopted in order to emphasize scenarios in which data communications face bad and good conditions and $\eta = 1$ is chosen. Furthermore, we use $\gamma = 10^{-2}$ because $\gamma \gg 10^{-2}$ would make the EH more advantageous than it really is. On the other hand, $\gamma \ll 10^{-2}$ results in very low values of harvested energy. Therefore, the chosen value of γ is the most realistic since it is closer to the real value of channel energy experienced by PLC channels.

Brief descriptions of the adopted NB-PLC and LP-RF wireless channel models are as follows.

NB-PLC Channel Model: We make use of the well-known Zimmermann and Dostert [35] channel model using the parameters taken from the IEEE 1901.2 standard [34, Annex D]. The additive noise in this NB-PLC channel is modeled as a zero mean colored Gaussian random process. Adopted from [36], its PSD is expressed by $\mathrm{S}^P(f) = \eta/2\exp(-\nu|f|)$, where $\nu, \eta \in \mathbb{R}_+$ are constants equal to 1.2×10^{-5} and 1.0×10^{-15}, respectively, and f is the frequency in Hertz. Given the subchannel bandwidth, $\Delta f = B_W/N$, we have that $\mathbf{\Lambda}_{\sigma^2_{\mathbf{v}_\ell^P}} = \Delta f\mathrm{diag}\{\mathrm{S}^P(0), \mathrm{S}^P(\Delta f), \ldots, \mathrm{S}^P([N-1]\Delta f)\}, \forall \ell$.

LP-RF Wireless Channel Model: We obtained this channel from a wideband wireless one by adopting the procedure suggested in the 802.15.4a IEEE wireless channel model report [37]. Essentially, it is accomplished by filtering the wideband wireless channel model. The zero-mean circularly symmetric complex Gaussian assumption is made for the wireless additive noise. From [38], the PSD of the additive noise in the wireless channel is considered to be $\mathrm{S}^W(f) = -173.8 + NF$ dBm/Hz, where the receiver noise figure NF is equal to 7 dB. As a result, we have that $\mathbf{\Lambda}_{\sigma^2_{\mathbf{v}_\ell^W}} = \Delta f\mathrm{diag}\{\mathrm{S}^W(0), \mathrm{S}^W(\Delta f), \ldots, \mathrm{S}^W([N-1]\Delta f)\}, \forall \ell$.

To carry out comparative numerical analyses, we will rely on the achievable data rate ratio, which is defined by

$$\varphi_b^a \triangleq \frac{C^a}{C^H} \tag{16}$$

$$\mathbf{C}_{\mathrm{AF}} = \mathrm{diag}\Bigg\{\mathbf{\Lambda}_{P_2^P}\mathbf{\Lambda}_{|\boldsymbol{\mathcal{H}}_{\mathrm{RD}}^P|^2}\mathbf{\Lambda}^{-1}_{\sigma^2_{\mathbf{Y}_{\mathrm{SR}}}}\left|\mathbf{D}^P\mathbf{\Lambda}_{\sqrt{P_1^P}}\boldsymbol{\mathcal{H}}_{\mathrm{SR}}^P + \mathbf{D}^W\mathbf{\Lambda}_{\sqrt{P_1^W}}\boldsymbol{\mathcal{H}}_{\mathrm{SR}}^W\right|^2 + \mathbf{\Lambda}_{P_2^W}\mathbf{\Lambda}_{|\boldsymbol{\mathcal{H}}_{\mathrm{RD}}^W|^2}\mathbf{\Lambda}^{-1}_{\sigma^2_{\mathbf{Y}_{\mathrm{SR}}}}\left|\mathbf{D}^P\mathbf{\Lambda}_{\sqrt{P_1^P}}\boldsymbol{\mathcal{H}}_{\mathrm{SR}}^P + \mathbf{D}^W\mathbf{\Lambda}_{\sqrt{P_1^W}}\boldsymbol{\mathcal{H}}_{\mathrm{SR}}^W\right|^2\Bigg\} \tag{12}$$

$$\mathbf{D}_{\mathrm{AF}} = \mathrm{diag}\Bigg\{\mathbf{\Lambda}_{P_2^P}\mathbf{\Lambda}_{|\boldsymbol{\mathcal{H}}_{\mathrm{RD}}^P|^2}\mathbf{\Lambda}^{-1}_{\sigma^2_{\mathbf{Y}_{\mathrm{SR}}}}\left(\left|\mathbf{D}^P\right|^2\mathbf{\Lambda}_{\sigma^2_{\mathbf{v}_{\mathrm{SR}}^P}} + \left|\mathbf{D}^W\right|^2\mathbf{\Lambda}_{\sigma^2_{\mathbf{v}_{\mathrm{SR}}^W}}\right) + \mathbf{\Lambda}_{\sigma^2_{\mathbf{v}_{\mathrm{RD}}^P}} + \mathbf{\Lambda}_{P_2^W}\mathbf{\Lambda}_{|\boldsymbol{\mathcal{H}}_{\mathrm{RD}}^W|^2}\mathbf{\Lambda}^{-1}_{\sigma^2_{\mathbf{Y}_{\mathrm{SR}}}}\left(\left|\mathbf{D}^P\right|^2\mathbf{\Lambda}_{\sigma^2_{\mathbf{v}_{\mathrm{SR}}^P}} + \left|\mathbf{D}^W\right|^2\mathbf{\Lambda}_{\sigma^2_{\mathbf{v}_{\mathrm{SR}}^W}}\right) + \mathbf{\Lambda}_{\sigma^2_{\mathbf{v}_{\mathrm{RD}}^W}}\Bigg\} \tag{13}$$

where C^a is the achievable data rate associated with the system a, where $a \in \{\text{H2HS, P2HS, W2HS}\}$ denotes the H2HS (any approach), P2HS, or W2HS model. Note that the source of power at the R node comes from the use of one of the aforementioned EH approaches. This means that each one of them uses the TS, PS, or HTS strategy and, as a consequence, we adopt $b \in \{\text{TS, PS, HTS}\}$. Also, C^H refers to the achievable data rate attained by the H2HS model by assuming a source of power at the R node and EH does not apply. In other words, this condition refers to a typical H2HS system.

Further, we assume that the complete channel state information is available at the transmitter side if optimal power allocation (OA) is applied by using the water-filling technique [39] at the S and R nodes. This technique optimally allocates the total transmission power among subcarriers based on knowledge of the normalized signal-to-noise ratio (nSNR) matrix, which can be expressed as $\mathbf{\Lambda}_{\overline{\zeta_\ell^q}} = \mathbf{\Lambda}_{|\boldsymbol{\mathcal{H}}_\ell^q|^2} \mathbf{\Lambda}^{-1}_{\sigma^2_{\mathbf{V}_\ell^q}} = \text{diag}\{\overline{\zeta_\ell^q}[0], \overline{\zeta_\ell^q}[1], \ldots, \overline{\zeta_\ell^q}[N-1]\}$ for the qth communication medium associated with the ℓth link, in which, for a given q and ℓ, $\overline{\zeta_\ell^q}[k]$ is the kth subchannel nSNR with $k \in \{0, 1, \ldots, N-1\}$ corresponding to the frequencies $f_k = k\Delta f$.

Past works have shown that the intrinsic PLC noise characteristic can increase the system performance when EH is adopted [30], [31]. Taking into account this issue, we perform the numerical analyses considering that the additive noise in the PLC channel can be white or colored. In this sense, the following four simulation settings are taken into account to support our quantitative analyses.

1) *Setting #1:* OA is used at the S and R nodes and the PLC channel output is corrupted by an additive colored Gaussian noise (ACGN).
2) *Setting #2:* OA is used at the S and R nodes. Also, the PLC channel is corrupted by additive white Gaussian noise (AWGN).
3) *Setting #3:* uniform power allocation (UA) is used at the S and R nodes and the PLC channel is disturbed by the presence of the ACGN.
4) *Setting #4:* UA is used at the S and R nodes, and the PLC channel is corrupted by AWGN.

Also, the four approaches for harvesting energy in the H2HS model (see Section III-C for more details) may be described as follows: if H2HS harvests the energy in the R node only from the wireless signal by means of the HTS strategy, then we call it Approach A; only from the power line signal and using the HTS strategy, Approach B; from both power line and wireless signals using the TS strategy, Approach C; and from both power line and wireless signals using the PS strategy, Approach D. Furthermore, the nonhybrid P2HS and W2HS models make use of the power line and wireless SR link, respectively, for EH and are straightforwardly associated with their acronyms.

A. Setting #1: OA, PLC Channel With ACGN

By considering Setting #1, Fig. 5 shows achievable data rate ratios as functions of the TS and PS factors, for Fig. 5(a) $P_S = 1$ mW and for Fig. 5(b) $P_S = 100$ mW. According to this plot, when $P_S = 100$ mW, there is a clear performance gap among H2HS (Approaches A, B, C, and D) and the nonhybrid dual-hop systems (P2HS and W2HS). This gap is in favor of H2HS and is irrelevant when $P_S = 1$ mW. As a matter of fact, if the transmission power is low, then the PLC portion has a greater contribution to the H2HS model than the WLC one and this behavior is less noticeable when the transmission power increases. Overall, this performance gap increase as P_S grows. For instance, when $P_S = 1$ mW, the optimal TS factor for the H2HS with Approach A and W2HS with TS is $\tau_{\text{OPT}} = 1/2$, which results in $\varphi_{\text{TS}}^{\text{W2HS}} = 0.06$ and $\varphi_{\text{HTS}}^{\text{H2HS}} = 0.18$ (Approach A). Therefore, $\varphi_{\text{HTS}}^{\text{H2HS}} - \varphi_{\text{TS}}^{\text{W2HS}} = 0.12$. For $P_S = 100$ mW and $\tau_{\text{OPT}} = 1/2$, we have $\varphi_{\text{HTS}}^{\text{H2HS}} - \varphi_{\text{TS}}^{\text{W2HS}} = 0.26$.

Regarding the use of the EH strategy in the H2HS model, we note that TS (Approach C) is better than PS (Approach D) for $\tau, \rho < 1/2$ and the opposite occurs for $\tau, \rho > 1/2$. Also, for any value of P_S and optimal values of τ and ρ, PS attains better performance than TS. In fact, unlike TS, the PS strategy does not affect the time interval reserved for the second phase. In other words, independent of the value of the PS factor, the PS strategy has T time interval for carrying out the R $\rightarrow$ D data communication, resulting in a tendency to increase the use of P_1 to perform EH rather than S $\rightarrow$ R data transmission during the first phase, which is confirmed by the high value of $\rho_{\text{OPT}} = 0.9$ in Approach D.

With the exception of energy, the characteristics of the channel that is used for EH do not exert influence on the amount of harvested energy. Therefore, for a given τ, the same energy is harvested in both Approaches A and B and they have the same performance in terms of the RD link usage. That said, the only difference between Approaches A and B is the use of power line and wireless SR links, respectively, which offers an advantage in favor of the PLC portion of the SR link when OA is adopted. In fact, OA can efficiently exploit the existing diversity of nSNR, which is associated with the effect of the frequency-selective PLC channel and nonflatness of the PSD. In other words, the characteristics of the PLC channel (i.e., channel frequency response and additive noise) cause OA to allocate the majority of P_1^P in a few subchannels (i.e., those showing the highest nSNR), something that does not happen in the wireless ones because the channel frequency response associated with the ISM band and the PSD are almost flat. Thus, Approach A offers better performance than Approach B in terms of SR link usage. Finally, the lack of matching among these few subchannels (i.e., they occupy distinct frequency bands) of the SR link and the RD link can cause the whole system to lose performance. This is the reason behind the improvement of Approach B over Approach A in Setting #1.

Moreover, for a given EH strategy, P2HS is better than W2HS for any value of the switching or splitting factor. In these cases, the PLC channels associated with SR and RD links share a large number of high nSNR subchannels, i.e., the high nSNR subchannels belonging to the SR and RD links are occupying the same frequency band due to the attenuation profile of the PLC channel frequency response. In other words, it is better to have subchannels associated with the

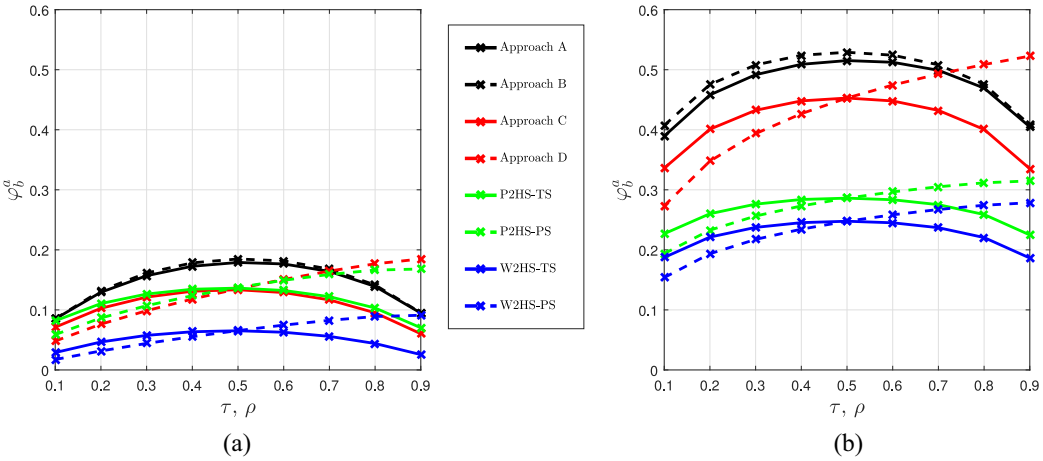

Fig. 5. Setting #1: φ_b^a versus τ, ρ for H2HS, P2HS, and W2HS with (a) $P_{\mathrm{S}} = 1$ mW and (b) $P_{\mathrm{S}} = 100$ mW.

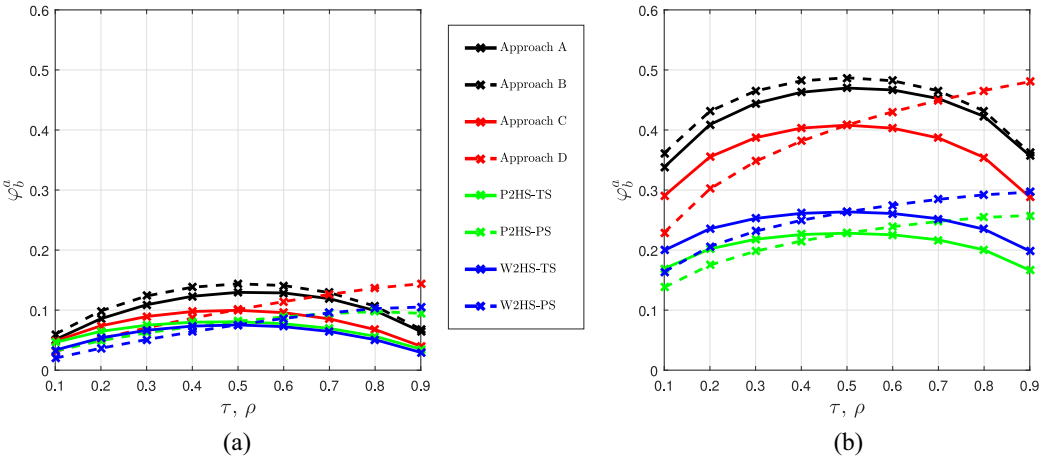

Fig. 6. Setting #2: φ_b^a versus τ, ρ for H2HS, P2HS, and W2HS with (a) $P_{\mathrm{S}} = 1$ mW and (b) $P_{\mathrm{S}} = 100$ mW.

SR link with low nSNR variation and subchannels associated with the RD link with high nSNR variation when operating in the Setting #1 conditions. Finally, we note that $\tau = 0$ and $\rho = 0$ are not feasible values since no energy would be harvested for the R $\rightarrow$ D data communication link. On the other hand, $\tau = 1$ and $\rho = 1$ would make data communication impossible.

B. Setting #2: OA, PLC Channel With AWGN

Fig. 6 shows achievable data rate ratios as functions of τ, ρ, for Fig. 6(a) $P_{\mathrm{S}} = 1$ mW and Fig. 6(b) $P_{\mathrm{S}} = 100$ mW, for Setting #2. Different from Setting #1, W2HS presents better performance than P2HS for any value of τ, ρ when $P_{\mathrm{S}} = 100$ mW. This occurs because, in this setting, the additive noise in the PLC channel has a flat PSD. In other words, one of the two advantages that P2HS offered in Setting #1 was removed (the other one is the high PLC frequency selectivity) because the difference between the nSNR variation in the PLC subchannels at both SR and RD links in comparison to the wireless ones is not as great as in Setting #1. However, with $P_{\mathrm{S}} = 1$ mW, P2HS yields similar performance to W2HS because the lower is the transmission power, the higher is the gain achieved by the use of OA in high frequency-selective channels [15].

Also, the nonflatness characteristic of the PSD of the additive noise in the PLC channel makes the absolute value of the achievable data rates higher than the flatness assumption related to the PSD of the PLC additive noise. For instance, the ratio between C^{P2HS} in Setting #1 and C^{P2HS} in Setting #2, results in more than 30% of improvement with $P_{\mathrm{S}} = 100$ mW and τ_{OPT}. Overall, H2HS and P2HS systems offer improvements in Setting #1 in relation to Setting #2. The exception is the W2HS system because it is not impacted by the assumption that the PSD of the additive noise of the PLC channel is flat.

C. Setting #3: UA, PLC Channel With ACGN

For Setting #3, the achievable data rate ratios as functions of τ, ρ, for $P_{\mathrm{S}} = 1$ mW and $P_{\mathrm{S}} = 100$ mW are shown in Fig. 7(a) and Fig. 7(b), respectively. By comparing $\varphi_{\mathrm{TS}}^{\mathrm{P2HS}}$ and $\varphi_{\mathrm{TS}}^{\mathrm{W2HS}}$ in Settings #3 (UA) and #1 (OA), we can notice that the change of the power resource allocation from OA to UA has a great and negative impact on the performance of the power line channels compared to the wireless ones. This occurs due

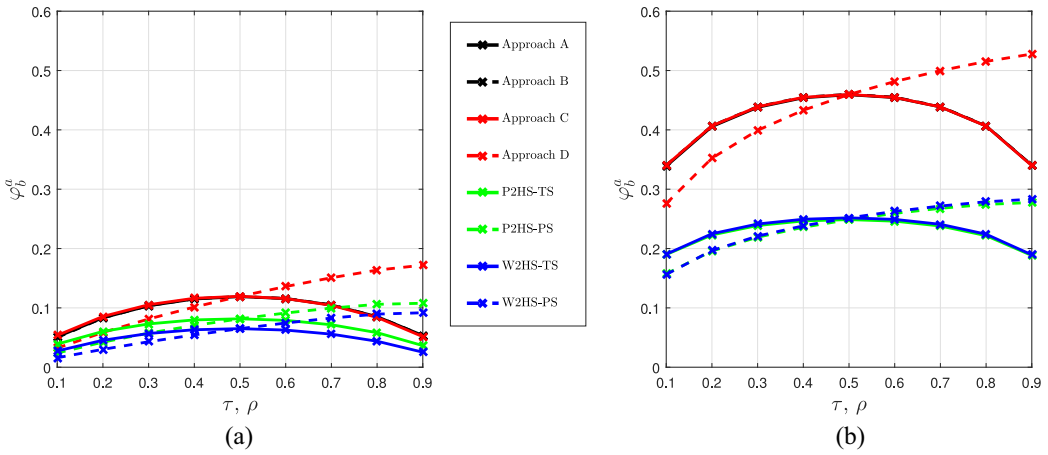

Fig. 7. Setting #3: φ_b^a versus τ, ρ for H2HS, P2HS, and W2HS with (a) $P_S = 1$ mW and (b) $P_S = 100$ mW.

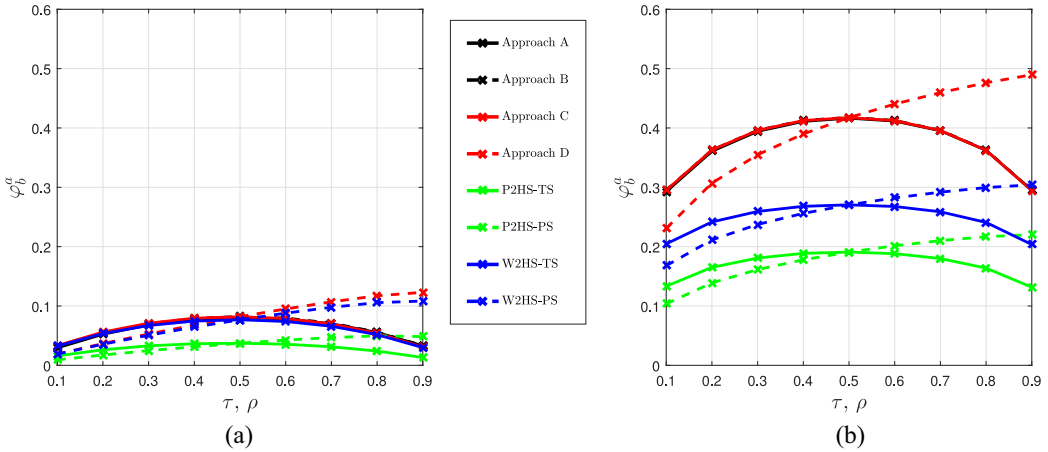

Fig. 8. Setting #4: φ_b^a versus τ, ρ for H2HS, P2HS, and W2HS with (a) $P_S = 1$ mW and (b) $P_S = 100$ mW.

to the high variation of the power line nSNR among subchannels. Therefore, when OA is adopted, the use of frequency selectivity of the nSNR of the power line channel is efficiently exploited, which does not happen when UA is applied. Due to that, in Setting #3, P2HS and W2HS have similar performances to the H2HS with wireless EH (Approach A) and the H2HS with power line EH (Approach B).

Different from what was noted with Settings #1 and #2, the performance of the H2HS model with power line or wireless EH (i.e., Approach A or B) is similar to that related to the H2HS with the TS (Approach C) strategy because both power line and wireless channels offer similar contributions to EH and achievable data rates in Setting #3. Further, the increase of P_S from 1 to 100 mW made the P2HS and W2HS performances even closer to each other due to the similar performance among subchannels, which is caused by the use of UA together with $\|\mathbf{h}_\ell^P\|^2 = \|\mathbf{h}_\ell^W\|^2$ and $P_{v,\ell}^W = P_{v,\ell}^P$.

D. Setting #4: UA, PLC Channel With AWGN

Regarding Setting #4, Fig. 8 shows achievable data rate ratios as functions of τ, ρ, for Fig. 8(a) $P_S = 1$ mW and Fig. 8(b) $P_S = 100$ mW. The lowest values of the achievable data rates for P2HS is noted in this setting. As a consequence, it leads to the greatest performance difference between P2HS and W2HS.

Concerning Setting #3, the change of behavior associated with P2HS is due to the noise assumption. In other words, if the PSD of the PLC additive noise is flat, then the power line channel frequency selectivity is more noticed than when the PSD of the additive noise is nonflat. As a matter of fact, the matching of the high nSNR subchannels in the SR and RD links is less frequent in the flat PSD than in the nonflat one. Besides, the nonflat PSD of PLC additive noise can result in more performance gain than the flatness of this PSD.

Furthermore, the change from OA (Setting #2) to UA (Setting #4) showed the flexibility of the W2HS and H2HS with mutual power line and wireless EH (Approaches C and D) to deal with the lack of OA, which is not present in P2HS and H2HS with the energy harvested from the power line or wireless signal (Approaches A and B). In fact, the change in the power allocation is more perceived in the power line channels than in the wireless ones when the additive PLC noise has a flat PSD. Also, Approaches A and B provide upper bounds for Approach C, regardless of the value of τ, ρ.

Moreover, Approach D with $\rho_{\mathrm{OPT}} = 0.9$ showed the best results in terms of achievable data rates. Also, Approach D is more resilient to a change of the PSD of the additive noise and the type of power allocation. In other words, Approach D appears to be more promising for implementation under the set of assumptions made. Overall, the results presented here support the use of H2HS together with an EH strategy for low-bit-rate applications, such as SG and IoT ones.

V. Conclusion

Based on EH principles, we have formulated the H2HS model in terms of achievable data rates. In this model, EH is performed at the relay node by using the HTS strategy (e.g., from the wireless signal—Approach A and the power line signal—Approach B), the TS strategy (Approach C), or the PS strategy (Approach D). Moreover, we have analyzed performance comparisons among the H2HS, P2HS, and W2HS models under four simulation settings.

Regardless of the EH strategy, we have shown that the H2HS model based on Approach D performs better than P2HS or W2HS in terms of the achievable data rate for any simulation setting. Thus, Approach D is more interesting for implementation due to its resilience against the type of power allocation and the PSD of the additive noise. Moreover, if the transmission power is high, then the nonflat PSD feature of the PLC additive noise at the channel output contributes to additional increase of the achievable data rate in comparison with the flatness of the PSD of the additive noise, which agrees with [30] and [31]. Also, we have found that optimal values of the TS and PS factors yield better performance in favor of the dual-hop system with the PS strategy rather than with the TS strategy. In addition, we have shown that Approaches A and B provide upper bounds for Approach C, for all assumptions and simulation settings.

Overall, we conclude that the hybridism concept can substantially benefit EH if the telecommunications systems demand energy efficiency and sustainability. As a consequence, the results of this paper offer considerable promise for SG and IoT applications and others, such as smart cities and Industry 4.0.

References

[1] S. Galli, A. Scaglione, and Z. Wang, "For the grid and through the grid: The role of power line communications in the smart grid," *Proc. IEEE*, vol. 99, no. 6, pp. 998–1027, Jun. 2011.

[2] A. Zanella, N. Bui, A. Castellani, L. Vangelista, and M. Zorzi, "Internet of Things for smart cities," *IEEE Internet Things J.*, vol. 1, no. 1, pp. 22–32, Feb. 2014.

[3] M. Nassar *et al.*, "Local utility power line communications in the 3–500 kHz band: Channel impairments, noise, and standards," *IEEE Signal Process. Mag.*, vol. 29, no. 5, pp. 116–127, Sep. 2012.

[4] T. R. Oliveira, A. A. M. Picorone, S. L. Netto, and M. V. Ribeiro, "Characterization of Brazilian in-home power line channels for data communication," *Elect. Power Syst. Res.*, vol. 150, pp. 188–197, Sep. 2017.

[5] M. de Lima Filomeno, G. R. Colen, L. G. de Oliveira, and M. V. Ribeiro, "Two-stage single-relay channel model for in-home broadband PLC systems," *IEEE Syst. J.*, to be published. [Online]. Available: https://ieeexplore.ieee.org/document/8416746/, doi: 10.1109/JSYST.2018.2852221.

[6] V. Fernandes, W. A. Finamore, M. V. Ribeiro, N. Marina, and J. Karamachoski, "Bernoulli–Gaussian distribution with memory as a model for power line communication noise," in *Proc. Braz. Telecommun. Signal Process. Symp.*, Sep. 2017, pp. 328–332.

[7] L. G. D. S. Costa, A. C. M. D. Queiroz, B. Adebisi, V. L. R. D. Costa, and M. V. Ribeiro, "Coupling for power line communications: A survey," *J. Commun. Inf. Syst.*, vol. 32, no. 1, pp. 8–22, Jan. 2017.

[8] M. Sayed, T. A. Tsiftsis, and N. Al-Dhahir, "On the diversity of hybrid narrowband-PLC/wireless communications for smart grids," *IEEE Trans. Wireless Commun.*, vol. 16, no. 7, pp. 4344–4360, Jul. 2017.

[9] J. Song *et al.*, "An indoor broadband broadcasting system based on PLC and VLC," *IEEE Trans. Broadcast.*, vol. 61, no. 2, pp. 299–308, Jun. 2015.

[10] M. Kashef, M. Ismail, M. Abdallah, K. A. Qaraqe, and E. Serpedin, "Energy efficient resource allocation for mixed RF/VLC heterogeneous wireless networks," *IEEE J. Sel. Areas Commun.*, vol. 34, no. 4, pp. 883–893, Apr. 2016.

[11] W. Jiang, T. Kaiser, and A. J. H. Vinck, "A robust opportunistic relaying strategy for co-operative wireless communications," *IEEE Trans. Wireless Commun.*, vol. 15, no. 4, pp. 2642–2655, Apr. 2016.

[12] M. S. P. Facina, H. A. Latchman, H. V. Poor, and M. V. Ribeiro, "Cooperative in-home power line communication: Analyses based on a measurement campaign," *IEEE Trans. Commun.*, vol. 64, no. 2, pp. 778–789, Feb. 2016.

[13] R. M. Oliveira, M. S. P. Facina, M. V. Ribeiro, and A. B. Vieira, "Performance evaluation of in-home broadband PLC systems using a cooperative MAC protocol," *Comput. Netw.*, vol. 95, pp. 62–76, Dec. 2015.

[14] Y. Qian *et al.*, "Design of hybrid wireless and power line sensor networks with dual-interface relay in IoT," *IEEE Internet Things J.*, to be published. [Online]. Available: https://ieeexplore.ieee.org/document/7973142/, doi: 10.1109/JIOT.2017.2725451.

[15] V. Fernandes, W. A. Finamore, H. V. Poor, and M. V. Ribeiro, "The low-bit-rate hybrid power line/wireless single-relay channel model," *IEEE Syst. J.*, to be published. [Online]. Available: https://ieeexplore.ieee.org/document/8187635/, doi: 10.1109/JSYST.2017.2775201.

[16] L. De Mello Brandao Abdo Dib, V. Fernandes, M. de Lima Filomeno, and M. V. Ribeiro, "Hybrid PLC/wireless communication for smart grids and Internet of Things applications," *IEEE Internet Things J.*, vol. 5, no. 2, pp. 655–667, Apr. 2018.

[17] V. Fernandes, H. V. Poor, and M. V. Ribeiro, "Analyses of the incomplete low-bit-rate hybrid PLC-wireless single-relay channel," *IEEE Internet Things J.*, vol. 5, no. 2, pp. 917–929, Apr. 2018.

[18] P. Kamalinejad *et al.*, "Wireless energy harvesting for the Internet of Things," *IEEE Commun. Mag.*, vol. 53, no. 6, pp. 102–108, Jun. 2015.

[19] X. Lu, P. Wang, D. Niyato, D. I. Kim, and Z. Han, "Wireless networks with RF energy harvesting: A contemporary survey," *IEEE Commun. Surveys Tuts.*, vol. 17, no. 2, pp. 757–789, 2nd Quart., 2015.

[20] I. Krikidis *et al.*, "Simultaneous wireless information and power transfer in modern communication systems," *IEEE Commun. Mag.*, vol. 52, no. 11, pp. 104–110, Nov. 2014.

[21] M. S. Omar, S. A. R. Naqvi, S. H. Kabir, and S. A. Hassan, "An experimental evaluation of a cooperative communication-based smart metering data acquisition system," *IEEE Trans. Ind. Informat.*, vol. 13, no. 1, pp. 399–408, Feb. 2017.

[22] V. C. Gungor *et al.*, "Smart grid technologies: Communication technologies and standards," *IEEE Trans. Ind. Informat.*, vol. 7, no. 4, pp. 529–539, Nov. 2011.

[23] L. Sun, P. Ren, Q. Du, and Y. Wang, "Fountain-coding aided strategy for secure cooperative transmission in industrial wireless sensor networks," *IEEE Trans. Ind. Informat.*, vol. 12, no. 1, pp. 291–300, Feb. 2016.

[24] L. R. Varshney, "Transporting information and energy simultaneously," in *Proc. IEEE Int. Symp. Inf. Theory*, 2008, pp. 1612–1616.

[25] P. Grover and A. Sahai, "Shannon meets Tesla: Wireless information and power transfer," in *Proc. IEEE Int. Symp. Inf. Theory*, 2010, pp. 2363–2367.

[26] A. A. Nasir, X. Zhou, S. Durrani, and R. A. Kennedy, "Relaying protocols for wireless energy harvesting and information processing," *IEEE Trans. Wireless Commun.*, vol. 12, no. 7, pp. 3622–3636, Jul. 2013.

[27] R. Zhang and C. K. Ho, "MIMO broadcasting for simultaneous wireless information and power transfer," *IEEE Trans. Wireless Commun.*, vol. 12, no. 5, pp. 1989–2001, May 2013.

[28] Z. Ding, S. M. Perlaza, I. Esnaola, and H. V. Poor, "Power allocation strategies in energy harvesting wireless cooperative networks," *IEEE Trans. Wireless Commun.*, vol. 13, no. 2, pp. 846–860, Feb. 2014.

[29] L. Elmorshedy and C. Leung, "Power allocation in an RF energy harvesting DF relay network in the presence of an interferer," *IEEE Access*, vol. 5, pp. 7606–7618, 2017.
[30] K. M. Rabie, B. Adebisi, A. M. Tonello, and G. Nauryzbayev, "For more energy-efficient dual-hop DF relaying power-line communication systems," *IEEE Syst. J.*, vol. 12, no. 2, pp. 2005–2016, Jan. 2017.
[31] K. M. Rabie and B. Adebisi, "Enhanced amplify-and-forward relaying in non-Gaussian PLC networks," *IEEE Access*, vol. 5, pp. 4087–4094, 2017.
[32] C. Choudhuri and U. Mitra, "Capacity bounds for relay channels with intersymbol interference and colored Gaussian noise," *IEEE Trans. Inf. Theory*, vol. 60, no. 9, pp. 5639–5652, Sep. 2014.
[33] A. J. Goldsmith and M. Effros, "The capacity region of broadcast channels with intersymbol interference and colored Gaussian noise," *IEEE Trans. Inf. Theory*, vol. 47, no. 1, pp. 219–240, Jan. 2001.
[34] *IEEE Standard for Low Frequency (Less Than 500 kHz) Narrow Band Power Line Communications for Smart Grid Application*, IEEE Standard 1901.2, 2013.
[35] M. Zimmermann and K. Dostert, "A multipath model for the power line channel," *IEEE Trans. Commun.*, vol. 50, no. 4, pp. 553–559, Apr. 2002.
[36] M. Katayama, T. Yamazato, and H. Okada, "A mathematical model of noise in narrowband power line communication systems," *IEEE J. Sel. Areas Commun.*, vol. 24, no. 7, pp. 1267–1276, Jul. 2006.
[37] A. F. Molisch *et al.*, "IEEE 802.15.4a channel model—Final report," IEEE 802.15 WPAN Low Rate Alternative PHY Task Group, Rep. IEEE 802.15-04-0662-02-004a, Nov. 2004.
[38] J.-H. Lee and Y.-H. Kim, "Diversity relaying for parallel use of power-line and wireless communication networks," *IEEE Trans. Power Del.*, vol. 29, no. 3, pp. 1301–1310, Jun. 2014.
[39] J. M. Cioffi. *Chapter 4: Multi-Channel Modulation*. Accessed: May 2016. [Online]. Available: http://web.stanford.edu/group/cioffi/book/chap4.pdf

Victor Fernandes received the B.S. and M.Sc. degrees in electrical engineering from the Federal University of Juiz de Fora, Juiz de Fora, Brazil, in 2015 and 2017, respectively, where he is currently pursuing the D.Sc. degree in electrical engineering.

His current research interests include signal processing, digital communication, smart grids, and Internet of Things.

H. Vincent Poor (S'72–M'77–SM'82–F'87) received the Ph.D. degree in electrical engineering and computer science from Princeton University, Princeton, NJ, USA, in 1977.

From 1977 to 1990, he was on the faculty of the University of Illinois at Urbana–Champaign, Urbana, IL, USA. Since 1990, he has been on the faculty at Princeton, where he is currently the Michael Henry Strater University Professor of Electrical Engineering. From 2006 to 2016, he served as the Dean of Princeton's School of Engineering and Applied Science. His current research interests include information theory and signal processing, and their applications in wireless networks, energy systems and related fields. Among his publications in these areas is the recent book *Information Theoretic Security and Privacy of Information Systems* (Cambridge Univ. Press, 2017).

Dr. Poor was a recipient of the Marconi and Armstrong Awards of the IEEE Communications Society in 2007 and 2009, respectively, and the 2017 IEEE Alexander Graham Bell Medal. He is a member of the National Academy of Engineering and the National Academy of Sciences and is a Foreign Member of the Chinese Academy of Sciences, the Royal Society and other national and international academies.

Moisés V. Ribeiro (S'03–M'05–SM'10) received the B.S. degree in electrical engineering from the Federal University of Juiz de Fora (UFJF), Juiz de Fora, Brazil, 1999, and the M.Sc. and D.Sc. degrees in electrical engineering from the University of Campinas, Campinas, Brazil, in 2001 and 2005, respectively.

He was a Visiting Scholar with the University of California at Santa Barbara, Santa Barbara, CA, USA, in 2004, a Visiting Professor from 2005 to 2007, and an Assistant Professor with UFJF from 2007 to 2015. Since 2015, he has been an Associate Professor with UFJF. He co-founded Smarti9 LTD., Juiz de Fora, and Wari LTD., in 2012 and 2015, respectively. He has authored over 170 peer-reviewed papers, 9 book chapters, and has filed 12 patents. His current research interests includes signal processing, digital communication, power line communication, smart grids, Internet of Things, and smart city.

Dr. Ribeiro was a recipient of the Fulbright Visiting Professorship at Stanford University, Stanford, CA, USA, in 2011, and at Princeton University, Princeton, NJ, USA, in 2012 and student awards of 2001 IEEE IECON and 2003 IEEE ISIE. He was the General Chair of 2010 IEEE ISPLC, 2013 IWSGC, SBrT 2015 and a Guest Co-Editor for special issues of the *EURASIP Journal on Advances in Signal Processing* and the *EURASIP Journal of Electrical and Computer Engineering*. He had served as the Secretary of the IEEE ComSoc TC-PLC.